Thermal modelling of battery configuration and self-discharge reactions in vanadium redox flow battery

Ao Tang, Jie Bao, Maria Skyllas-Kazacos*

School of Chemical Engineering, University of New South Wales, Sydney, NSW 2052, Australia

HIGHLIGHTS

► Precipitation of vanadium ions occurs at low or high electrolyte temperature.
► Vanadium ion diffusion leads to self-discharge and capacity loss.
► Self-discharge reactions release heat into the supporting electrolyte.
► Mathematical modelling can help with predicting the variation in electrolyte temperature and the loss of capacity.
► Temperature and rebalancing control systems can be developed based on the model to optimize the battery operation.

ARTICLE INFO

ABSTRACT

During the operation of vanadium redox flow battery, the vanadium ions diffuse across the membrane as a result of concentration gradients between the two half-cells in the stack, leading to self-discharge reactions in both half-cells that will release heat to the electrolyte and subsequently increase the electrolyte temperature. In order to avoid possible thermal precipitation in the electrolyte solution and prevent possible overheating of the cell components, the electrolyte temperature needs to be known. In this study, the effect of the self-discharge reactions was incorporated into a thermal model based on energy and mass balances, developed for the purpose of electrolyte temperature control. Simulations results have shown that the proposed model can be used to investigate the thermal effect of the self-discharge reactions on both continuous charge–discharge cycling and during standby periods, and can help optimize battery designs and fabrication for different applications.

1. Introduction

The all-vanadium redox flow battery (VFB) is a typical electro-chemical energy storage system which was initially invented by Skyllas-Kazacos and co-workers at University of New South Wales (UNSW) dating back to the 1980s [1,2]. Studies on the VFB began at UNSW and subsequently proceeded in Japan, UK, China and elsewhere covering a wide range of topics. With a number of successful field trials and applications around the world, the development of VFBs has to date reached commercial fruition and been regarded as one of the most suitable large-scale energy storage solutions. The VFB stores energy chemically in external reservoirs, while the redox reactions take place at inert electrode in the cell stack. The capacity and the power rating can therefore be independently designed by selection of stack size for the required power rating and electrolyte volume for kWh capacity. Other than its flexibility for scale-up, most of the competitive features of the VFB are associated with the use of the same element in both half-cells, thus effectively eliminating the cross contamination over extended charge–discharge operation. Several other major advantages include high energy efficiency, long life cycle and low capital cost.

Despite the elimination of cross contamination in the vanadium redox flow battery however, the diffusion of different ions across the membrane inevitably takes place due to the concentration gradients between the two half-cell electrolytes during charge–discharge cycling. While the crossover of hydrogen ions carries the current and helps facilitate the electron transfer reactions, the diffusion of the different vanadium ions will give rise to self-discharge which subsequently leads to capacity loss. Such a loss of capacity in the VFB can be restored by simply remixing the electrolytes periodically. In addition to the capacity loss however, the self-discharge processes also release heat which can accumulate in the cell stack and increase the electrolyte temperature.

* Corresponding author. Tel.: +61 2 9385 4335; fax: +61 2 9385 5966.
E-mail address: m.kazacos@unsw.edu.au (M. Skyllas-Kazacos).

Nomenclature

A	surface area (m^2)		
A_0	pre-factor		
C_p	specific heat (J g^{-1} K^{-1})		
c	vanadium concentration (mol L^{-1})		
d	membrane thickness (m)		
E_a	activation energy (J mol^{-1})		
F	Faraday's constant (C mol^{-1})		
H	change of enthalpy (J mol^{-1})		
I	charging or discharging current (A)		
k	diffusion coefficient (m^2 s^{-1})		
N	number of cells		
Q	flow rate (L s^{-1})		
r	overall stack resistance (Ω)		
R	gas constant (J mol^{-1} K^{-1})		
S	electrode area (m^2)		
T	temperature (°C)		
U	overall heat transfer coefficient (W m^{-2} K^{-1})		
V	volume (L)		
W	thermal power (J s^{-1})		
z	electros involved in the redox reaction		

Greek symbol

ρ	electrolyte density (g L^{-1})

Superscript

s	stack
t	tank

Subscript

(1)	self-discharge reaction (1)
(2)	self-discharge reaction (2)
(4)	self-discharge reaction (4)
(5)	self-discharge reaction (5)
2	V^{2+}
3	V^{3+}
4	VO^{2+}
5	VO_2^+
air	surrounding air
n	negative side
p	positive side
pipe	pipe
pump	pump
p1−	pipe connected to the pump at negative side
p2−	pipe at the negative side
p1+	pipe connected to the pump at positive side
p2+	pipe at the positive side
s and stack	stack

Although flow batteries have an advantage over conventional batteries of having a built-in heat exchanger that can extract heat from the cell stack during electrolyte circulation, severe heat accumulation in the cell stack could occur during standby periods when the pumps are switched off, or during slow charge–discharge cycles when there is an inadequate electrolyte flow rate. As a result, thermal precipitation of VO_2^+ in the positive electrolyte could occur if the electrolyte temperature exceeds a certain limit that depends on the vanadium electrolyte concentrations [3]. Any thermal precipitation of VO_2^+ in the positive electrolyte would not only further contribute to capacity loss, but potential blockage of the electrolyte channels could restrict flow into the cells, leading to premature voltage cut-off during operation.

Apart from the thermal precipitation of VO_2^+, studies also have shown that V^{2+} could be precipitated in the negative electrolyte at lower electrolyte temperatures, depending on the vanadium concentration used. The electrolyte temperature therefore, plays a crucial role in the performance of the VFB. Varying electrolyte temperature can influence the rate of ion diffusion associated with the membrane property which, in turn, impacts on the amount of heat released by the self-discharge reactions. In practice, the electrolyte temperature can be significantly affected by the surrounding temperature, battery materials and design. It is therefore, vital to manage the electrolyte temperature within the optimal range by designing the batteries and choosing the electrolyte composition to suit the climatic conditions for the specific installation. This is currently achieved by diluting the vanadium electrolyte concentration and limiting the operational state-of-charge range of the battery to prevent any one of the vanadium oxidation states from exceeding their respective solubility limit over the expected temperature range in the specific location. These actions often result in an unnecessary reduction in energy density of the system however, leading to greater footprint or building space. By implementing a sophisticated temperature control system, however, these problems can be avoided.

Mathematical modelling of the all-vanadium redox flow battery can assist in analysing the battery performance under different operating and climatic conditions for the purpose of optimal battery design and control system development. Electrochemical modelling of the cells was initially carried out by Walsh et al., followed by a number of extended models on different aspects [4–6] such as concentration and temperature gradients within the cell. While these models are useful for predicting cell voltage profiles, they are not suitable for studying the dynamic control or operation of VFBs. These models also neglected the effect of ion diffusion and hydrogen evolution on capacity loss during extended cycling. Skyllas-Kazacos and co-workers recently presented a dynamic model capable of revealing the capacity loss caused by ion diffusion [7] and gassing side reactions by incorporating Fick's law into the material balance equations [8]. Such a model may help the implementation of periodic electrolyte rebalancing. A thermal model of the VFB was also proposed to investigate the variations in electrolyte temperature during extended charging–discharging cycling, as affected by the heat generated inside the stack and exchanged with the surroundings [9]. This model provides flexibility for different VFB designs and environmental conditions and its potential to be employed in the development of a model-based controller for the VFB systems makes it viable to eliminate the precipitation by controlling the electrolyte temperature during operation. The heat released by the self-discharge processes due to the diffusion of vanadium ions across the membrane was not considered in development of the above thermal model however, nor was the impact of electrolyte temperature on the rate of ion diffusion taken into account in the previous study on capacity loss.

In this paper, the thermal model is further developed by coupling the energy balance of the self-discharge reactions with the mass balances that reveal the crossover of vanadium ions through the membrane. Thus, the interaction of vanadium ion diffusion and self-discharge heat is correlated. This coupled model is able to not only predict more precisely the electrolyte temperature, but indicate the level of capacity loss as well. Furthermore, such a model will be useful for both electrolyte temperature control and capacity restoration management that can help optimize the battery performance and enhance the efficiency.
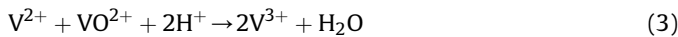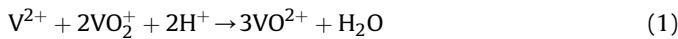
2. Mathematical model development

In this section, the self-discharge reactions caused by ion diffusion are firstly discussed in detail, followed by the assumptions made in effort to assist in developing the dynamic model. Mass and energy balances are then applied to model the concentrations of vanadium ions in each of the four oxidation states and the electrolyte temperature in both the stack and tanks. The interaction of the electrolyte temperature and the rate of diffusion is linked by means of introducing a serious of self-discharge reaction heat terms in the energy balances and employing the varying diffusion rates derived empirically as a function of temperature in the mass balances.
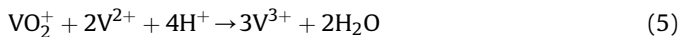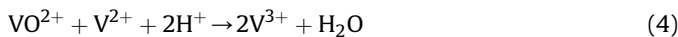
2.1. Ion diffusion and self-discharge reactions

As an exclusive feature of the VFB, cross contamination is prevented by the use of the same element in both half-cells such that the VFB endows a theoretically infinite life cycle. Ion diffusion across the membrane, nevertheless, still takes place since the membrane acts as a separator that allows the specific ions to transfer between the two half-cell electrolytes to balance the charge. Ideally, the membrane employed in the VFB ought to enable hydrogen ions to go through the membrane while preventing the transfer of vanadium ions from one half-cell to the other. In reality, however, the diffusion of vanadium ions cannot be fully avoided as a consequence of concentration gradients that exist at all times during charge–discharge cycling or standby. As a result, a series of self-discharge reactions associated with the diffusion of each vanadium ion will occur and subsequently lead to a loss of capacity and heat generation in the cell stack. Potential thermal precipitation of VO_2^+ in the stack could occur if the VFB experiences a shutdown for an extended period of time during which the heat released from the self-discharge reactions can be accumulated inside the cell stack. This can give rise to further capacity loss and possibly block the electrolyte channels with resultant flow restrictions when the pumps are restarted. In the VFB, the self-discharge reactions are given as follows [10]:

In the positive half-cell, V^{2+} and V^{3+} diffused from the negative side will react with VO^{2+} and VO_2^+:

$$V^{2+} + 2VO_2^+ + 2H^+ \rightarrow 3VO^{2+} + H_2O \tag{1}$$

$$V^{3+} + VO_2^+ \rightarrow 2VO^{2+} \tag{2}$$

$$V^{2+} + VO^{2+} + 2H^+ \rightarrow 2V^{3+} + H_2O \tag{3}$$

In the negative half-cell, diffusion of VO^{2+} and VO_2^+ from the positive side will react with V^{2+} and V^{3+}:

$$VO^{2+} + V^{2+} + 2H^+ \rightarrow 2V^{3+} + H_2O \tag{4}$$

$$VO_2^+ + 2V^{2+} + 4H^+ \rightarrow 3V^{3+} + 2H_2O \tag{5}$$

$$VO_2^+ + V^{3+} \rightarrow 2VO^{2+} \tag{6}$$

2.2. Basic assumptions for modelling

In order to derive the dynamic model from conservation of mass and energy for the VFB, the following assumptions were made:

(1) The electrolyte is fully filled in the tank;
(2) Self-discharge reactions are instantaneous;

(3) Reactions described in Eqs. (3) and (6) are negligible;
(4) The concentration and temperature in each tank, pipe and cell (or stack) are uniform;
(5) The stack and tanks behave as continuous stirred tank reactors (CSTRs);
(6) Stack resistance remains constant over the operating state-of-charge range of the VFB.

In terms of gassing side reactions, the evolution of hydrogen at the negative electrode can be eliminated by operating the VFB at below 100% state-of-charge while the oxidation of V^{2+} at the positive side can be minimized by employing an inert gas blanket in the negative electrolyte tank to exclude oxygen, and/or by designing the tank with a small electrolyte surface area to volume ratio to make the air oxidation process diffusion limited. In this study, the oxidation of V^{2+} is neglected based on assumption (1), while the effect of hydrogen evolution is considered in the charging current applied. Side reactions (3) and (6) are neglected since these two reactions generate V^{3+} and VO^{2+} respectively that further react with VO_2^+ and V^{2+} respectively, thus giving the same net reactions as reactions (1) and (5).

2.3. Mass balance for vanadium ions

In order to quantify the transfer of vanadium ions through the membrane, Fick's law is adopted to develop the mass balance equations. In general, the pipe volume is normally quite small compared to the volumes of the tank and stack. Therefore, mass balance in the pipes is neglected in the mass balance model. As the heat transfer via the pipes is taken into account in this paper, the energy balance in the pipes is considered in the thermal model. Each of the four different oxidation states of the vanadium ions is modelled for the tank and stack based on conservation of mass as follows:

For V^{2+} ion

$$\frac{V_{stack}}{2}\frac{dc_2^s}{dt} = Q_n(c_2^t - c_2^s) \pm \frac{NI}{zF} - Nk_2(T_{stack})\frac{c_2^s}{d}S$$
$$- 2Nk_5(T_{stack})\frac{c_5^s}{d}S - Nk_4(T_{stack})\frac{c_4^s}{d}S \tag{7}$$

$$V_n\frac{dc_2^t}{dt} = Q_n(c_2^s - c_2^t) \tag{8}$$

For V^{3+} ion

$$\frac{V_{stack}}{2}\frac{dc_3^s}{dt} = Q_n(c_3^t - c_3^s) \mp \frac{NI}{zF} - Nk_3(T_{stack})\frac{c_3^s}{d}S$$
$$+ 3Nk_5(T_{stack})\frac{c_5^s}{d}S + 2Nk_4(T_{stack})\frac{c_4^s}{d}S \tag{9}$$

$$V_n\frac{dc_3^t}{dt} = Q_n(c_3^s - c_3^t) \tag{10}$$

For VO^{2+} ion

$$\frac{V_{stack}}{2}\frac{dc_4^s}{dt} = Q_p(c_4^t - c_4^s) \mp \frac{NI}{zF} - Nk_4(T_{stack})\frac{c_4^s}{d}S$$
$$+ 3Nk_2(T_{stack})\frac{c_2^s}{d}S + 2Nk_3(T_{stack})\frac{c_3^s}{d}S \tag{11}$$

$$V_p\frac{dc_4^t}{dt} = Q_p(c_4^s - c_4^t) \tag{12}$$

For $VO2^+$ ion

$$\frac{V_{\text{stack}}}{2}\frac{dc_5^s}{dt} = Q_p(c_5^t - c_5^s) \pm \frac{NI}{zF} - Nk_5(T_{\text{stack}})\frac{c_5^s}{d}S$$
$$- 2Nk_2(T_{\text{stack}})\frac{c_2^s}{d}S - Nk_3(T_{\text{stack}})\frac{c_3^s}{d}S \qquad (13)$$

$$V_p\frac{dc_5^t}{dt} = Q_p(c_5^s - c_5^t) \qquad (14)$$

All the variables in above equations can refer to the Nomenclature. As the membrane properties are affected by the surrounding electrolyte temperature in the stack, the permeability varies such that the diffusion coefficients depend on the stack temperature. The temperature dependence of diffusion coefficients can be modelled by the following Arrhenius equation:

$$k = A_0 e^{-E_a/RT} \qquad (15)$$

where A_0 is the pre-factor, R is the universal gas constant and E_a is the activation energy for diffusion.

2.4. Energy balance

To investigate the variation in electrolyte temperature, energy balance equations for the tanks, stack and pipes are developed based on the conservation of energy. Depending on the type of pumps used, heat from the pumps could impact on the electrolyte temperature to some extent. In addition to the consideration of heat transfer at the pipes, the effect of self-discharge reactions on the energy balance in the stack is also introduced into the present model. This will allow simultaneous simulation of electrolyte temperature and individual vanadium ion concentrations in order to predict whether self-discharge reactions in the stack during standby could lead to possible thermal precipitation of VO_2^+ in the positive half-cells if there is insufficient heat transfer between the stack and the environment. Such predictions would assist in optimal stack material selection and design.

The detailed energy balance equations are described as follows:
For the stack

$$C_p\rho V_{\text{stack}}\frac{dT_{\text{stack}}}{dt} = Q_p C_p\rho(T_{p1+} - T_{\text{stack}}) + Q_n C_p\rho(T_{p1-} - T_{\text{stack}})$$
$$+ U_s A_s(T_{\text{air}} - T_{\text{stack}}) + I^2r + Nk_2(T_{\text{stack}})\frac{c_2^s}{d}S$$
$$\cdot\left(-\Delta H_{(1)}\right) + Nk_3(T_{\text{stack}})\frac{c_3^s}{d}S\cdot\left(-\Delta H_{(2)}\right)$$
$$+ Nk_4(T_{\text{stack}})\frac{c_4^s}{d}S\cdot\left(-\Delta H_{(4)}\right) + Nk_5(T_{\text{stack}})\frac{c_5^s}{d}S$$
$$\cdot\left(-\Delta H_{(5)}\right) \qquad (16)$$

where $\Delta H_{(1)}$, $\Delta H_{(2)}$, $\Delta H_{(4)}$ and $\Delta H_{(5)}$ are the changes of enthalpy corresponding to self-discharge reactions (1), (2), (4) and (5), which were calculated based on the enthalpy of vanadium compound at 298.15 K shown in Table 1, and I^2r is the rate of heat generation by the stack resistance. As the current and stack resistance are not constant during charge–discharge cycling, the value of term I^2r will vary. For the purpose of the present study however, it is assumed that the stack resistance is constant over the operating state-of-charge range of the battery.

Eq. (16) is only valid when V^{2+}, V^{3+}, VO^{2+} and VO_2^+ all exist, such as in the process of charge–discharge cycling. In the case of standby VFB systems, long-term idle will cause either V^{2+} and/or VO^{2+} ions to be eventually depleted in the cells depending on the diffusion rates as a consequence of self-discharge reactions. Therefore, the terms of heat of reactions need to be adjusted accordingly. If V^{2+} is depleted ahead of VO_2^+, the reaction heat term will be determined

Table 1
Enthanlpies of formation of vanadium species at 298.15 K [12,13].

Formula	State	ΔH/kJ mol⁻¹
V^{2+}	Aqueous	(−226)
V^{3+}	Aqueous	(−259)
VO^{2+}	Aqueous	−486.8
VO_2^+	Aqueous	−649.8
H_2O	Aqueous	−285.8
H^+	Aqueous	0

NOTE: The values in parentheses are estimated.

by Eqs. (2) and (6) occurring in the positive and negative side respectively. In contrast, if VO_2^+ is completely consumed first, the heat of reaction will be decided by Eqs. (3) and (4). Meanwhile, the flow rate and current become zero in this case. Thus, Eq. (16) can be modified as follows:

If V^{2+} is depleted and VO_2^+ still exists in the stack

$$C_p\rho V_{\text{stack}}\frac{dT_{\text{stack}}}{dt} = U_s A_s(T_{\text{air}} - T_{\text{stack}})$$
$$+ Nk_3(T_{\text{stack}})\frac{c_3^s}{d}S\cdot\left(-\Delta H_{(2)}\right)$$
$$+ Nk_5(T_{\text{stack}})\frac{c_5^s}{d}S\cdot\left(-\Delta H_{(2)}\right) \qquad (17)$$

If VO_2^+ is depleted and V^{2+} still exists in the stack

$$C_p\rho V_{\text{stack}}\frac{dT_{\text{stack}}}{dt} = U_s A_s(T_{\text{air}} - T_{\text{stack}})$$
$$+ Nk_4(T_{\text{stack}})\frac{c_4^s}{d}S\cdot\left(-\Delta H_{(4)}\right)$$
$$+ Nk_2(T_{\text{stack}})\frac{c_2^s}{d}S\cdot\left(-\Delta H_{(4)}\right) \qquad (18)$$

After both V^{2+} and VO_2^+ are depleted in the stack, only V^{3+} and VO^{2+} remain and diffuse through the membrane until the concentrations are balanced. In the end, both positive and negative electrolyte will contain equal amounts of V^{3+} and VO^{2+} which is normally referred as the $V^{3.5+}$ oxidation state [11].

For the tank and pipes at the positive side, we have:

$$C_p\rho V_{\text{pipe}}\frac{dT_{p1+}}{dt} = Q_p C_p\rho(T_p - T_{p1+}) + U_{\text{pipe}}A_{\text{pipe}}(T_{\text{air}} - T_{p1+})$$
$$+ W_{\text{pump}} \qquad (19)$$

$$C_p\rho V_p\frac{dT_p}{dt} = Q_p C_p\rho(T_{p2+} - T_p) + U_p A_p(T_{\text{air}} - T_p) \qquad (20)$$

$$C_p\rho V_{\text{pipe}}\frac{dT_{p2+}}{dt} = Q_p C_p\rho(T_{\text{stack}} - T_{p2+}) + U_{\text{pipe}}A_{\text{pipe}}(T_{\text{air}} - T_{p2+})$$
$$\qquad (21)$$

where T_{p1+} is the electrolyte temperature in the pipe through which the electrolyte is pumped from the tank to the positive half-cells in the stack, and T_{p2+} is the electrolyte temperature in the other sections of the pipe in which the electrolyte solution is pushed back to the tank by pressure (See Fig. 1). It is also assumed that the two individual parts of pipe at positive or negative side have the same dimensions such that the volumes are identical.

2.4.1. For the tank and pipes at negative side

$$C_p\rho V_{\text{pipe}}\frac{dT_{p1-}}{dt} = Q_n C_p\rho(T_n - T_{p1-}) + U_{\text{pipe}}A_{\text{pipe}}(T_{\text{air}} - T_{p1-})$$
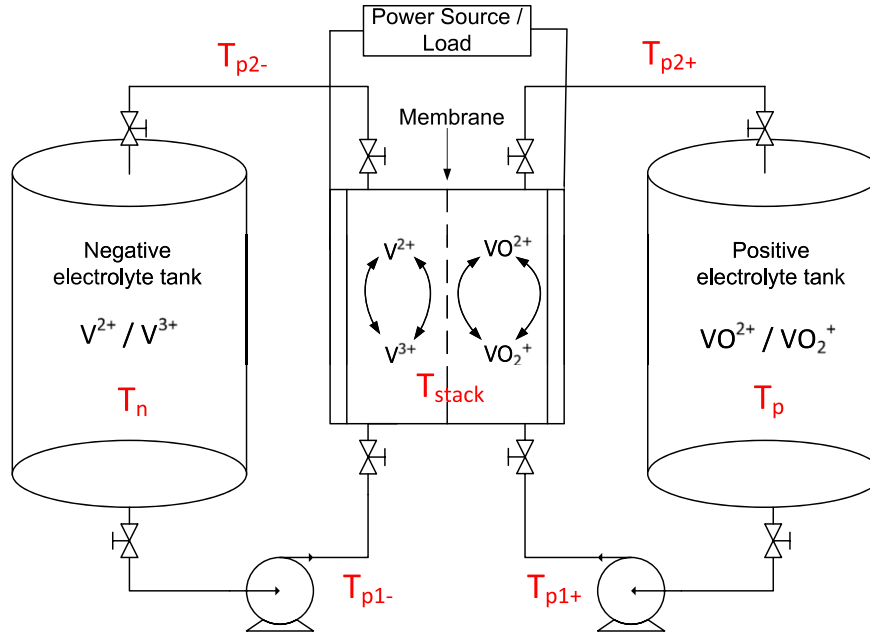$$+ W_{\text{pump}} \qquad (22)$$

Fig. 1. Diagram of the electrolyte temperature at each part of the VFB.

$$C_p \rho V_n \frac{dT_n}{dt} = Q_n C_p \rho (T_{p2-} - T_n) + U_n A_n (T_{air} - T_n) \qquad (23)$$

$$C_p \rho V_{pipe} \frac{dT_{p2-}}{dt} = Q_n C_p \rho (T_{stack} - T_{p2-}) + U_{pipe} A_{pipe} (T_{air} - T_{p2-}) \qquad (24)$$

If the tanks and pipes for the positive and negative sides of the battery are designed with the same specifications, the parameters in Eqs. (22)–(24) will be identical to those in Eqs. (19)–(21). Furthermore, the rate of pump heating W_{pump} is determined by the type of pumps and its operating conditions. This information can be obtained from the relevant pump specifications manual. As mentioned previously, for the purpose of the present study, it was assumed that magnetically coupled pumps are used in the VFB and that these transfer negligible heat to the electrolyte.

3. Simulation and results

3.1. Parameters

The specification of the VFB and the parameters employed in the simulations are listed in Table 2. The VFB system consisting of 19 identical cells in the stack has a nominal rating of 2.5 kW/15 kWh. The electrolyte solutions of each half-cell have a volume of 250 L calculated on the basis of an average cell voltage of 1.4 V and a concentration of 2 M vanadium in 4.4 M total sulphate, being separated by a Nafion membrane 115 [14]. It is assumed that the temperature dependence of the diffusion coefficients follows the Arrhenius equation as shown in Eq. (15). Referring to the data in Ref. [14], the temperature dependence of the diffusion coefficient for VO^{2+} ion was determined by least squares approximation. The activation energy and pre-factor were calculated as 17,341 J mol^{-1} and 0.0041 respectively. Correspondingly, the temperature dependence of the diffusion coefficients for the other three vanadium ions was derived using the assumption that the activation energy is the same for each of the species. The average cell resistivities for charging and discharging are assumed to be constant

Table 2
Specifications of the VFB and parameters in the simulation.

Parameters	Value	Reference
Total vanadium concentration, c	2 mol L^{-1}	
Specific heat capacity of electrolyte, C_p	3.2 J g^{-1} K^{-1}	[9,15]
Electrolyte density, ρ	1.354 g cm^{-3}	[9,16]
Number of cells, N	19	
Charging average cell resistivity, r_c	2 Ω cm^2	[11]
Discharging average cell resistivity, r_d	2.2 Ω cm^2	[11]
Membrane area, S	1500 cm^2	
Faraday's constant, F	96,485 C mol^{-1}	
Number of electrons transferred, z	1	
Enthalpy change of reaction (1), $\Delta H_{(1)}$	−220 kJ mol^{-1}	
Enthalpy change of reaction (2), $\Delta H_{(2)}$	−64 kJ mol^{-1}	
Enthalpy change of reaction (4), $\Delta H_{(4)}$	−91.2 kJ mol^{-1}	
Enthalpy change of reaction (5), $\Delta H_{(5)}$	−246.8 kJ mol^{-1}	
Diffusion coefficient of V^{2+}, k_2	5.261 × 10^{-6} cm^2 min^{-1} (25 °C)	[14]
Diffusion coefficient of V^{3+}, k_3	1.933 × 10^{-6} cm^2 min^{-1} (25 °C)	[14]
Diffusion coefficient of VO^{2+}, k_4	4.095 × 10^{-6} cm^2 min^{-1} (25 °C)	[14]
Diffusion coefficient of VO_2^+, k_5	3.538 × 10^{-6} cm^2 min^{-1} (25 °C)	[14]
Thickness of the membrane, d	1.27 × 10^{-4} m	
Overall heat transfer capability of the tank, $U_n × A_n$ (and $U_p × A_p$)	12.69 J K^{-1}s^{-1}	
Overall heat transfer capability of the stack, $U_s × A_s$	1.31 J K^{-1}s^{-1}	
Overall heat transfer capability of the pipe, $U_{pipe} × A_{pipe}$	0.47 J K^{-1}s^{-1}	
Electrode surface area	1500 cm^2	
Dimension of each cell	30 × 50 × 0.6 cm^3	
Tank height	1 m	
Tank radius	0.276 m	
Tank thickness	0.01 m	
Pipe length	1 m	
Pipe radius	0.02 m	
Pipe thickness	0.004 m	
Thermal conductivity of polypropylene	0.16 W m^{-1}K^{-1}	[17]
Thermal conductivity of stainless steel	16.3 W m^{-1}K^{-1}	[17]

during the operation, which are chosen to be 2 Ω cm^2 and 2.2 Ω cm^2 respectively [11]. Gassing side reactions are considered by assuming that 1% loss of current at the negative electrode goes into hydrogen evolution during charging. It is further assumed that the negative electrolyte tank has a nitrogen blanket so that air oxidation of V^{2+} may be neglected.

The stack is assumed to be made of polypropylene flow-frames with both polypropylene and stainless steel end plates where the thicknesses of the inner polypropylene plates and the outer steel plates are 20 mm and 10 mm respectively. Except for the end plates, the thicknesses of other sides (formed by the stacked flow-frames) are all set to be 50 mm as shown in Fig. 2. It is also assumed that the two cylindrical electrolyte tanks have the same size and four pipes with the same dimension are employed to connect the tanks and the stack. Both the pipes and the tanks are made of polypropylene. In order to investigate the variations in temperature at each element, it is assumed that the electrolyte solution of each half side fully fills the stack, the tank and the two pipes, and is separated by valves during standby periods such that the interaction of temperature can be eliminated.

Heat transfer to the atmosphere occurs at the stack, the pipes and the two electrolyte tanks. For different material thicknesses, shapes and surface areas of the components, the derivation of the overall heat transfer coefficient varies. In the simulations, the convective heat transfer refers to the calculations in our previous work [9], while the conductive heat transfer can be calculated on the basis of the thickness and thermal conductivity of the respective layer. The overall heat transfer capability of each component is therefore a sum of overall heat transfer coefficients multiplied by the corresponding surface area at that specific component. The values for the three components have been calculated and are listed in Table 2.

The time-varying flow rate is calculated as twice of the theoretical flow rate, depending on the magnitude of the current, the total vanadium concentration and the state-of-charge (or state-of-discharge) according to Faraday's law. In the process of charging, the state-of-discharge is derived on the basis of the minimum tank concentration of V^{3+} and VO^{2+}, as an imbalance caused by differential rates of ion diffusion exists [8]. Likewise, the calculation of state-of-charge is based on the minimum tank concentration of V^{2+} and VO$_2^+$ in discharging. By employing time-varying flow rate, energy wasted at the pump can be minimized so that the total

energy efficiency is improved. The effect of pump heat loss on the electrolyte temperature is assumed to be negligible in this study, as the lining in the pump head is usually thick and made of low thermal conductivity materials such as polypropylene and most of heat would be dissipated to the atmosphere directly via the metal pump body. Finally, the surrounding air temperature is approximated by the following sine-squared relationship:

$$T_{air} = B \cdot \sin^2(\omega t + \varphi) + C \qquad (25)$$

where (B + C) = maximum temperature reached; C = minimum temperature reached; ω = angular frequency, rad s^{-1}; ϕ = phase, rad; t = time, s.

3.2. Simulation of self-discharge in a back-up scenario

To investigate the effect of self-discharge on the electrolyte temperature in the stack, the 2.5 kW/15 kWh VFB is simulated in an emergency back-up power system application after being charged from 20:00 until 90% state-of-charge is achieved. At this point, the pumps are switched off and the system remains on standby. For the purpose of the present simulation, no float charging is included. It is assumed that the VFB is operated in a hot climate and the highest temperature in a day occurs at 14:00 at noon as shown in Fig. 3. With a charging current of 40 A, the electrolyte temperature in the stack is 25 °C after the first charging. Afterwards, self-discharge will gradually proceed and release heat to the electrolyte in the stack. Concentration polarization at the electrolyte-membrane surface tends to become larger in the case where the VFB is sitting without electrolyte flow through the cell stack. As it has however been reported in Ref. [10] that the vanadium ion diffusion coefficients in the solution are two magnitudes larger than through the Nafion 115 membrane. It is therefore possible to assume that the concentration gradient for the vanadium ions occurs only across the membrane and that the solution concentrations do not vary with distance from the membrane surface.

Fig. 4 indicates the variation in vanadium concentrations in the stack during the self-discharge process for 4 days. With the Nafion membrane employed in the simulation, it can be observed that the V^{2+} ions in the negative half-cell are depleted after approximately 6 h, while the remaining VO$_2^+$ ions in the positive half-cell are about 0.2 mol L^{-1}. From this moment on, only reactions (2) and (6) will
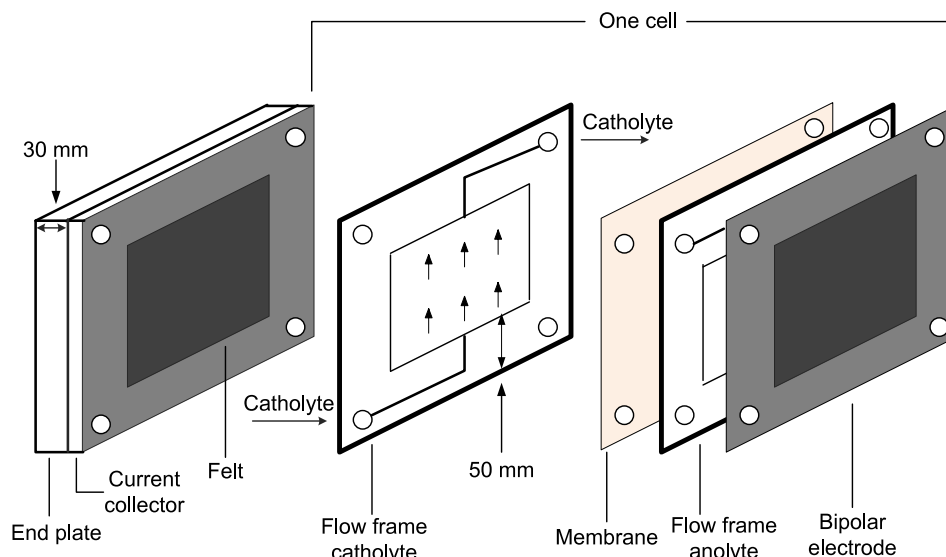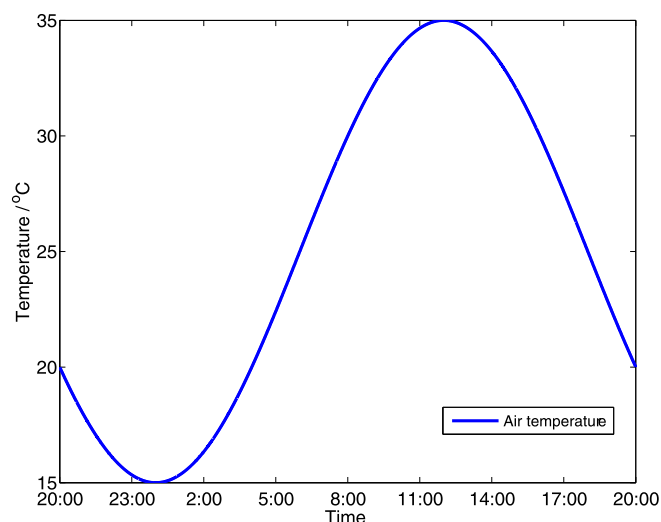
Fig. 2. Basic components of a redox cell.

Fig. 3. The surrounding air temperature profile.

Fig. 5. The variations in stack electrolyte temperature with insulate and non-insulated stack during the standby period.

occur in the positive and negative electrolyte respectively until the remaining VO_2^+ ions are completely reacted. During this period, VO^{2+} ions in the positive half-cell will start diffusing and accumulate in the negative half-cell electrolyte. After the remaining VO_2^+ depleted, V^{3+} will start emerging in the positive side and eventually approaches steady state within 4 days. It is apparent that the concentration gradient of V^{3+} vanishes faster than that of VO^{2+} ions, which is consistent with the order of magnitudes of the diffusion coefficients listed in Table 2.

The variation of stack temperature during the self-discharge process is plotted in Fig. 5. As the stack is non-insulated, the stack temperature is affected by both air temperature and self-discharge heating. It is observed from the blue line that the stack temperature starts to increase to approximately 58 °C when both V^{2+} and VO_2^+ disappear in the stack, followed by a decrease attributed to the heat exchange to the atmosphere. After 3 days, the stack temperature is shown to be stabilized and oscillates around 25 °C with the same frequency as the surrounding air temperature. If the stack is designed to have a poor heat transfer capability, the stack electrolyte tempera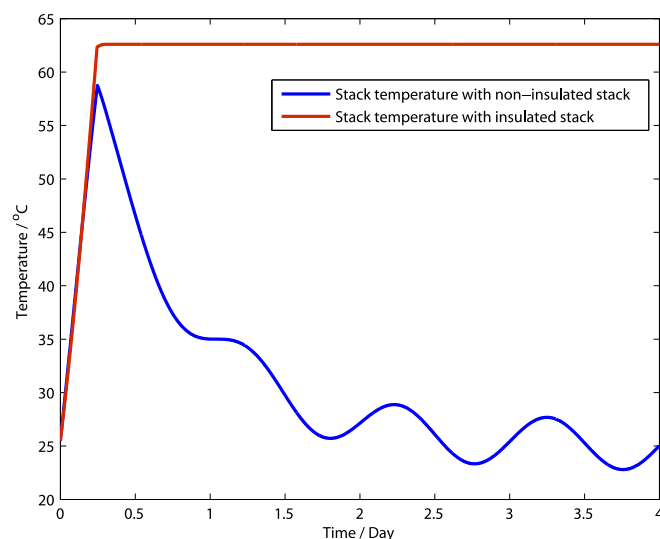ture will approach steady state more slowly. The worst scenario can be seen from the red curve in Fig. 5, where the stack temperature levels off at approximately 63 °C with an insulated stack design. It is known that thermal precipitation of VO_2^+ could occur for electrolytes containing 2 M or higher VO_2^+ ions if the electrolyte temperature exceeds 40 °C. Nevertheless, in the present scenario, no thermal precipitation will take place within the stack for either case since the concentration of VO_2^+ ions has dropped to below 1 M due to the self-discharge reactions by the time the stack temperature has reached 40 °C. This may not be the case for the solution within the internal electrolyte channels however, where ion concentration changes would be controlled by slower diffusion processes within the long, narrow channels. The risk of thermal precipitation may still be present in the channels therefore if there is no heat transfer between the stack and the cooler air and this would lead to undesirable blockages and flow restrictions within the channels.

3.3. Simulation of a residential power arbitrage scenario

3.3.1. VFB with Nafion membrane

To investigate the variation in electrolyte temperature during charging–discharging cycling, a residential power arbitrage scenario was simulated using the proposed models. In this simulation, the VFB system is used for peak shaving during the peak hours (14:00–20:00) with an operating range of 10–90% SOC. The charging period starts after 20:00 when a low electricity tariff rate is offered. To avert a long additional idle period after charging, the charging current was chosen to be 40 A on the basis of Faraday's law of electrolysis. As the charging proceeds, an imbalance between V^{2+} and VO_2^+ emerges due to the vanadium ion diffusion and self-discharge reactions occur gradually, making the states-of-charge of the two half-cells imbalanced. The process of charging ceases if either of the SOCs of the two half-cell electrolytes reaches 90% prior to 14:00, and the battery remains on standby until discharge at a constant current of 80 A for peak shaving at 14:00. The discharging ends when the SOC of either of the two half-cells reaches 10% prior to 20:00. After that, the VFB experiences an idle period till 20:00 when charging is restarted. If the SOCs do not reach 10% at 20:00, the VFB will be switched to charging mode regardless of the SOCs in order to take advantage of low electricity tariffs. During the standby periods, the pumps are switched off and heat is released
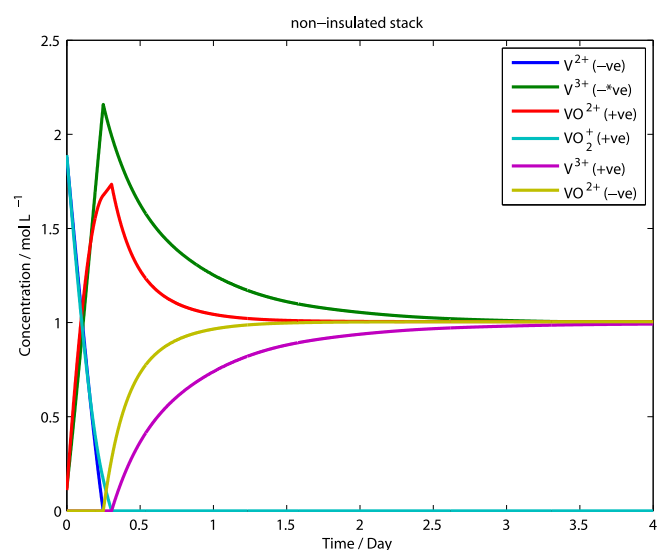

Fig. 4. The variations in stack concentrations of vanadium ions during the standby period.

inside the stack by the self-discharge reactions across the membrane. The variation of the surrounding air temperature in Fig. 3 is also applied in this case. The initial electrolyte temperatures in both the tanks and the stack are thus set to 20 °C corresponding to the air temperature at 20:00.

The current and flow rate profiles in the 1st day are shown in Fig. 6(a) and (b). As expected, the charging time is longer than the theoretical value while the discharging time is shorter in each cycle as a result of self-discharge. In long-term operation, however, both charging and discharging times will gradually decrease day by day. This can be attributed to the loss of capacity caused by the different rates of vanadium ion diffusion and self-discharge reactions. The varying flow rate can save unnecessary energy waste of the pump and meanwhile ensure that there is adequate supply of reactant species to the cell for the redox reactions occurring with the given current.

The rate of heat generation and stack voltage profiles are given in Fig. 6(c) and (d) respectively. The rate of heat generation from the self-discharge processes is quite small compared with heat generated from the stack resistance. The self-discharge reactions are, however, the only source of heat release during idle periods, and this gives rise to the increase in electrolyte temperature as can be seen in Fig. 7. Despite the very low rate of heat generation from the self-discharge reactions, however, it is worth noting that the stack temperature can jump up to 40 °C when the pumps are switched off during the standby period, which makes the heat accumulate gradually in the stack. The sudden drop in stack temperature can be observed when the VFB starts to discharge, as the pumps are turned on that makes the electrolyte circulate to dissipate the heat accumulated in the stack.

Fig. 8 reveals the variation of V^{2+} and V^{3+} concentrations on the negative side of the battery during the 1st operating day, while Fig. 9 presents the tank and stack concentration profiles for all the four vanadium ions in the stack and tanks. The rapid increase and decrease in the stack concentrations can be observed at the
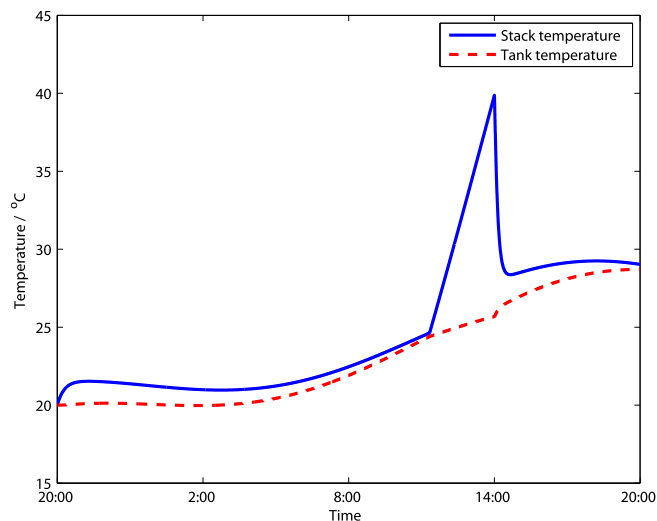

Fig. 7. The variation in stack and tank temperatures in the 1st day.

beginning of charging and discharging, due to the small flow rate when charging and discharging initiate as shown in Fig. 6(b). The tank concentration profile for the 1st week is shown in Fig. 10. It is evident that an imbalance in SOCs of the two half-cell electrolytes emerges as a result of differential rates of vanadium ion diffusion across the membrane and particularly hydrogen evolution in the negative electrolyte, leading to a subsequent loss of capacity of approximately 5.6% after operating for 1 week. In long-term operation, this capacity loss will continue to take place and thus influence the performance of the battery. With the prediction of the presenting model, actions for rebalancing the cell and SOC correction may however be implemented periodically to restore the capacity of the battery system.
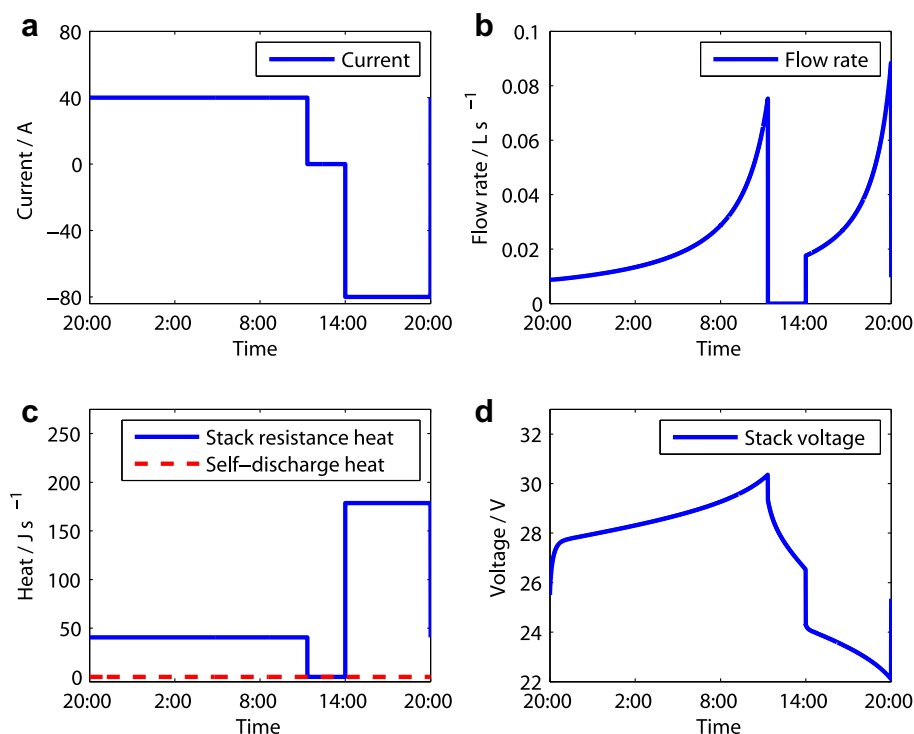

Fig. 6. (a) One-day profile of current, (b) flow rate, (c) heat generation and (d) stack voltage.
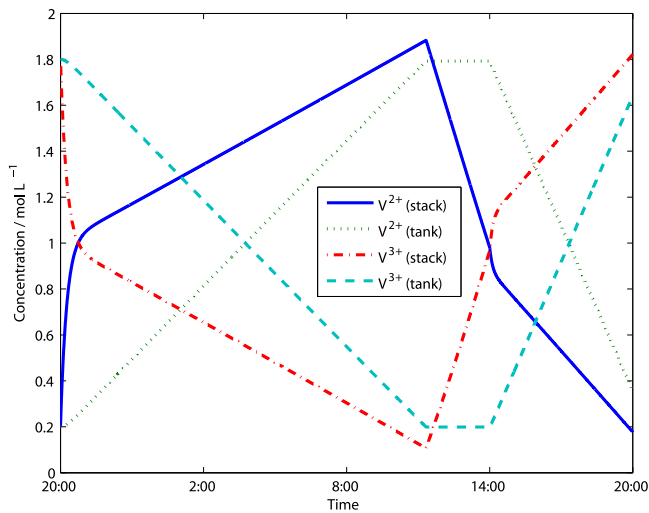
Fig. 8. The variation in vanadium concentration in the negative half-cell in the 1st day.

Fig. 10. Tank concentration profile for 7 days.

The trends of electrolyte temperatures in the stack and the tank for the 1st week are presented in Fig. 11. It can be seen that the electrolyte temperature in the stack can jump to 50 °C during the long standby period after charging, because the heat released by the self-discharge reactions continues to accumulate in the stack. Nonetheless, no thermal precipitation of VO_2^+ is likely to occur in the tank in the relatively hot climate assumed in this simulation, since the tank electrolyte temperatures oscillates around 30 °C. Furthermore, despite the jump in stack temperature to above 50 °C during the standby period as a result of heat from self-discharge reactions, thermal precipitation of VO_2^+ should not take place in the stack either, because of the drop in VO_2^+ concentration as
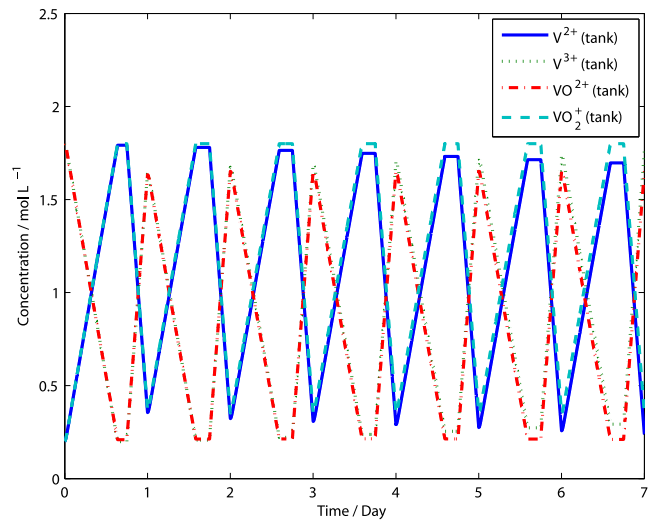
a consequence of continuous self-discharge. Unlike the situation with the standby application where the battery is left in the charged state for very long periods of time, the daily cycling of the battery in the power arbitrage application will preclude any precipitation in the channels because of the relatively long induction time associated with the VO_2^+ thermal precipitation reaction [18]. The corresponding stack voltage profile is presented in Fig. 12, where a fast drop in voltage can be observed after the VFB is charged, which is due to the self-discharge that influences the concentration ratio of each half-cell electrolyte. The following sudden drop in voltage primarily arises from the restart of discharging when the flowing electrons in the stack lead to the IR
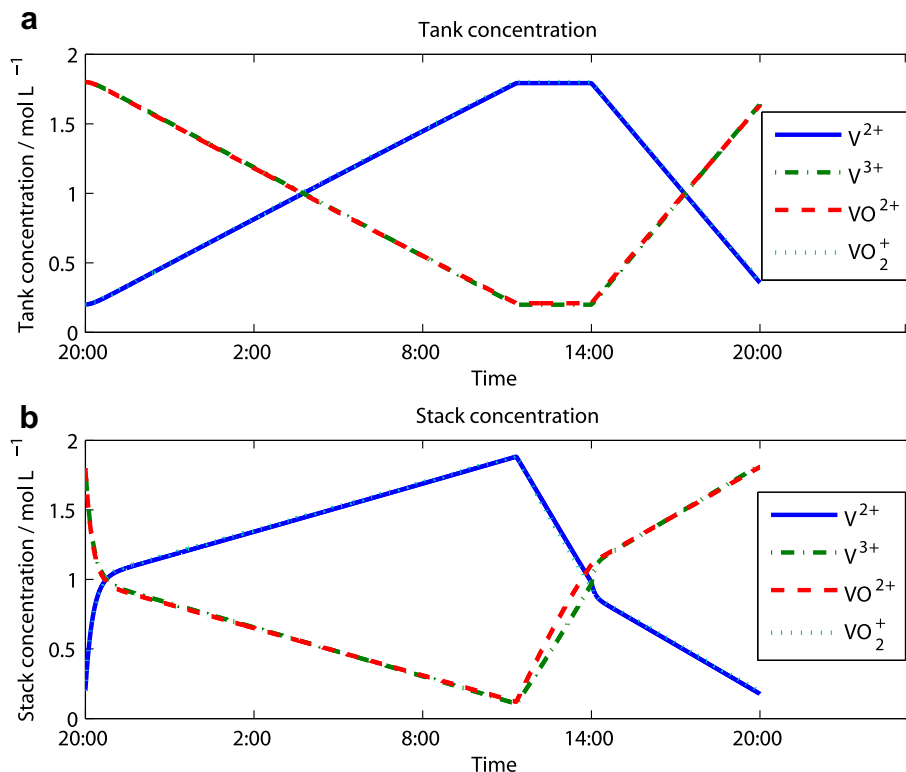

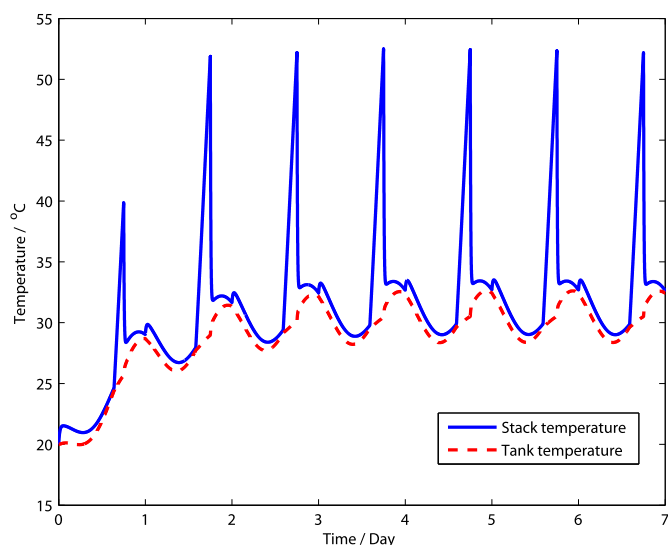Fig. 9. The tank and stack concentrations profile for the 1st day.

Fig. 11. The variation of electrolyte temperature in both the stack and the tank in 7 days.

drop. Initially the stack voltage reflects the concentrations of the vanadium ions in the cell stack that reflect a lower SOC than the tank electrolytes due to the self-discharge processes across the membrane. Once the stack electrolyte is replaced by fresh solution from the tanks, however, the stack voltage will increase slightly in response to the higher SOC of the solutions entering the stack. Furthermore, it can be estimated from the voltage profile that an average power output of 1.8 kW can be achieved for this residential power arbitrage scenario.

3.3.2. Effect of membrane properties on thermal balance

In the previous simulations, Nafion was selected as the membrane for the cell stack due to the availability of vanadium ion permeability values for the determination of self-discharge rates. Despite the widespread study of Nafion membranes for VFB applications however, the high cost of Nafion has precluded their use in commercial systems. Furthermore, the high degree of swelling of Nafion membranes in aqueous solutions gives rise to

high degrees of permeability for the vanadium ions and high rates of water transfer across the membrane. While considerable work has been done to overcome these problems by membrane modification [19,20], other types of membranes are currently used in commercial VRB systems and improved membranes are also undergoing development [21,22].

Although data for these membranes is currently unavailable, it is reasonable to assume that the optimal VRB membrane has been chosen on the basis of low permeability to vanadium ions. For more realistic simulations of the VFB in different applications, therefore it was assumed that the membrane has one-tenth diffusion coefficients of the Nafion membrane. Using this assumption, the concentration profiles in the negative electrolyte are illustrated in Fig. 13. As expected, the self-discharge rate during the standby period is much shorter than that for the VRB stack with Nafion membrane as indicated by the stack concentrations of the different vanadium ions. The corresponding electrolyte temperature variations are plotted in Fig. 14. It can be observed that the stack temperature during the standby period does not increase dramatically in this case and the electrolyte temperature oscillates stably around 27 °C. For real-life VFB systems, it is therefore expected that the Nafion membrane would be replaced by a low cost membrane with low permeability to achieve the optimal performance, so this is a more realistic prediction of VRB self-discharge and thermal balance.

3.3.3. Effect of electrolyte flow rate

To investigate the effect of volumetric flow rate on battery performance, a constant flow rate calculated on the basis of a minimum SOC of 20% during discharge and twice the theoretical flow rate was employed in the simulation as shown in Fig. 15. As the fast flow rate delivers vanadium ions into the stack at a much higher rate from the beginning of discharging, it can be observed that the initial discharging stack voltage is higher than that of with a varying flow rate, thereby possibly delivering more power during discharge. Under this circumstance, however, more energy will be consumed by the pumps during the operation. In practical VFB applications, therefore, the trade-off should be considered between the pump loss and the power efficiency.

Fig. 16 demonstrates the corresponding concentration and temperature profiles. It is observed that the lower stack concentration of V^{2+} caused by the self-discharge, jumps back to a very
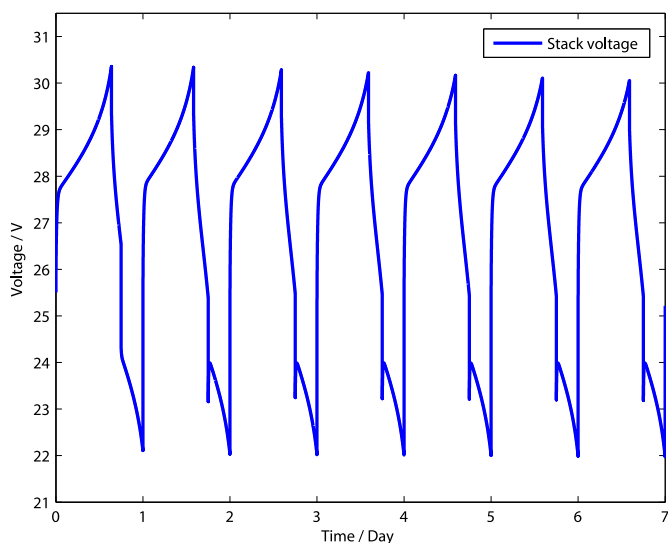

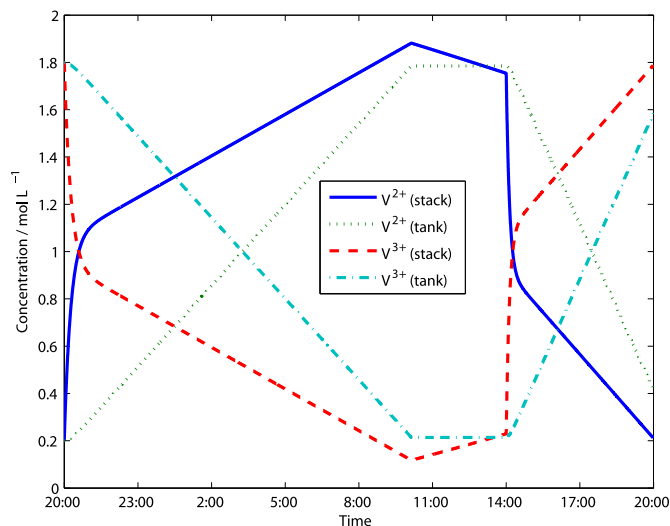**Fig. 12.** Stack voltage profile for 7 days.

Fig. 13. The concentration variations in the negative electrolyte with one-tenth diffusion coefficients of Nafion membrane.
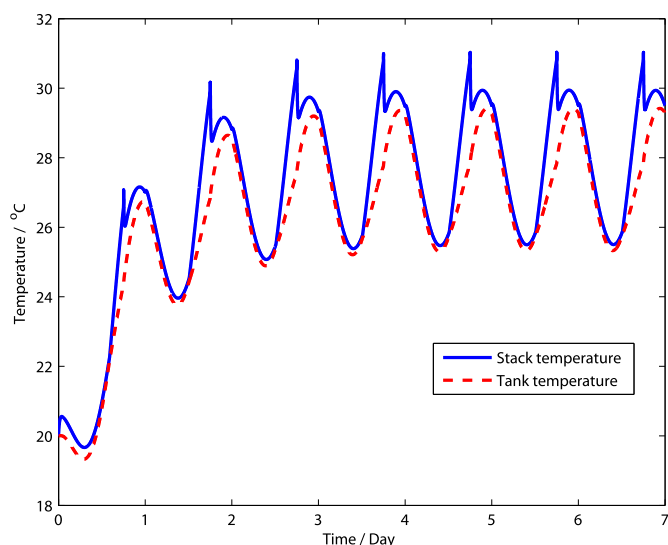
Fig. 14. The electrolyte temperature variation with one-tenth diffusion coefficients of Nafion membrane.

high level when discharging initiates. Under such a fast constant flow rate that provides good heat transfer capability, the temperature difference between the tank and the stack is quite small during charging—discharging cycling, while imposing negligible influence on stack temperature during the standby period.

3.4. Discussion

Simulations have shown that the proposed model is capable of predicting the effect of self-discharge reactions on the electrolyte temperature in the stack. This is particularly useful in the case of emergency back-up VFB systems where the VFB will experience

relatively long-term standby periods, so it is critical to select appropriate materials and stack design to eliminate any potential problems of internal heat accumulation. In order to develop the present model however, certain assumptions were made that could overestimate the degree of self-discharge and subsequent temperature rises. In particular, despite the assumption that the ion concentrations are uniform in each half-cell, concentration gradients always exist at the membrane—electrolyte interface in reality. During the charging and discharging processes, the concentration polarization can be limited to a relative thin layer at the membrane surface due to the flow of the solution. The thickness of the boundary layer at the membrane electrolyte surface can be larger in the back-up battery scenario however due to no electrolyte flow in the cell stack. The diffusion rates are, therefore, likely to differ from those obtained from the permeation experiments in which the electrolyte is pumped from the small measuring cylinder to the dialysis cell. As the diffusion rates constantly vary with the experimental conditions, it is difficult to quantify dynamically. Thus, the constant empirical value from the experiment is suitable for being employed in the simulation for different scenarios in spite of the error that exists.

In this work, the temperature dependence of the diffusion coefficient links the energy balance to the mass balance, which provides a more accurate prediction and a deeper insight into the determination of the varying diffusion coefficients for the model. The Arrhenius equation is a simple formula that can be used to model the temperature dependence of the diffusion rates in the presence of experimental data. The unknown parameters in Arrhenius equation can be determined by least squares approximation using the experimental diffusion rates obtained at different temperatures.

The other parameter that will affect the use of simulation results in real-life VFB systems is electrolyte composition. Thermal precipitation of VO_2^+ in the positive electrolyte could take place at elevated electrolyte temperature, owing to the inherently endothermic nature of the following precipitation reaction:
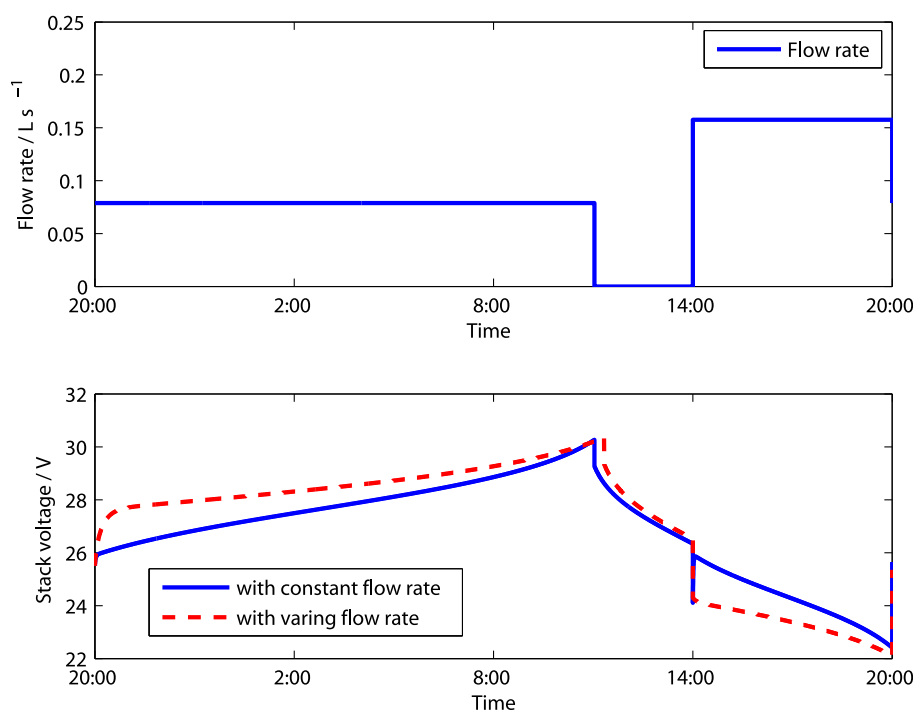

Fig. 15. Constant flow rate and the corresponding stack voltage profiles.
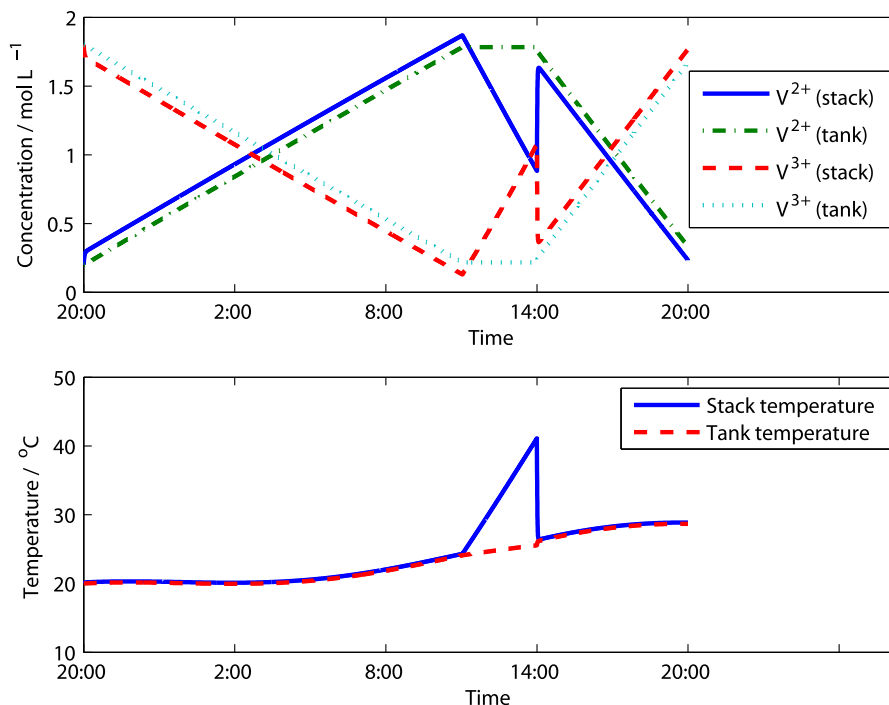
Fig. 16. The concentration and temperature profiles with a constant flow rate.

$$2VO_2^+ + H_2O \rightarrow V_2O_5 + 2H^+ \tag{26}$$

Theoretically, using high concentrations of sulphuric acid can help reduce the possible thermal precipitation occurring at elevated temperature by shifting the equilibrium for reaction (26) towards the left and hence increase the upper temperature limit for the VFB. It is however, not viable in reality since the stability of V^{2+}, V^{3+} and VO^{2+} ions at low temperature can be reduced in high concentration of sulphuric acid. Furthermore, the electrode and the membrane properties could also be harmed by extreme temperatures. A temperature control system is, therefore, required to be incorporated to regulate the surrounding temperature of the VFB system.

In practice, the VFB system is normally stored in a room or a box along with an air-conditioner or heat exchanger being used to adjust the surrounding temperature. Due to the unknown electrolyte temperature inside the VFB, the temperature control without any guidance can be energy inefficient. By using the mathematical model to predict the electrolyte temperature, more targeted control action can be applied to achieve tight temperature control. Unlike our previous thermal model [9], the proposed model considers the heat from self-discharge reactions such that it can forecast the variation in electrolyte temperature during slow charge–discharge cycling and standby period. Moreover, the model can be employed to develop a model-based control system to monitor and control the electrolyte temperature during both the series of cycles and the standby period. Last but not least, the development of the proposed model can also provide an insight into the VFB configuration and design, such as the choices of the material and the tank dimension in accordance with the climate of the application site.

4. Conclusion

A thermal model coupled with mass balance equations is proposed to investigate the thermal effect of self-discharge on electrolyte temperature. The energy balance has incorporated the heat generated by the self-discharge reactions whose rate of reaction is coupled with the diffusion term in mass balance equations. The diffusion coefficients in mass balance equations are also considered to be a function of the stack temperature from the energy balance. In this way, the heat of self-discharge reactions can be modelled as a function of both stack temperature and concentrations.

A 2.5 kW/15 kWh VFB system is simulated for use of peak shaving and back-up cases. Simulation results have shown that the heat of self-discharge reactions can contribute significantly to the increase of electrolyte temperature during the standby periods, while being negligible in the process of charging or discharging where the heat released from the stack resistance has a dominant impact on total heat generation and the electrolyte flow also plays an important role in heat transfer and dissipation. Besides, the comparison of the simulation results has also highlighted the importance of the membrane permeability in real-life VFB systems. The Nafion membrane can be employed in laboratory trials, but needs to be replaced by alternative membranes that have low vanadium permeability and low cost in large-scale real-life VFB applications. The proposed model can be used to develop a model-based temperature battery control system and improve the battery designs for different application requirements.

References

[1] M. Skyllas-Kazacos, M. Rychcik, R.G. Robins, A.G. Fane, M.A. Green, J. Electrochem. Soc. 133 (1986) 1057–1058.
[2] M. Skyllas-kazacos, M. Rychick, R. Robins, All-vanadium redox battery, United States Patent, No. 4,786,567, 1988.
[3] F. Rahman, M. Skyllas-Kazacos, J. Power Sources 189 (2009) 1212–1219.
[4] A.A. Shah, M.J. Watt-Smith, F.C. Walsh, Electrochim. Acta 53 (2008) 8087–8100.
[5] H. Al-Fetlawi, A.A. Shah, F.C. Walsh, Electrochim. Acta 55 (2009) 78–89.
[6] D. You, H. Zhang, J. Chen, Electrochim. Acta 54 (2009) 6827–6836.
[7] M. Skyllas-Kazacos, L. Goh, J. Memb. Sci. 399–400 (2012) 43–48.
[8] A. Tang, J. Bao, M. Skyllas-Kazacos, J. Power Sources 196 (2011) 10737–10747.
[9] A. Tang, S. Ting, J. Bao, M. Skyllas-Kazacos, J. Power Sources 203 (2012) 165–176.
[10] D. You, H. Zhang, C. Sun, X. Ma, J. Power Sources 196 (2011) 1578–1585.

[11] T. Sukkar, M. Skyllas-Kazacos, J. Appl. Electrochem. 34 (2004) 137–145.
[12] M.J. LaSalle, J.W. Cobble, J. Phys. Chem. 59 (1955) 519–524.
[13] C. Blanc, Modelling of a vanadium redox flow battery electricity storage system, Ph.D. Thesis, EPFL, Switzerland, 2009.
[14] C. Sun, J. Chen, H. Zhang, X. Han, Q. Luo, J. Power Sources 195 (2010) 890–897.
[15] R.H. Perry, G. Green, Perry's Chemical Engineers' Handbook, sixth ed., McGraw-Hill International Editions, 1984.
[16] A. Mousa, Chemical and electrochemical studies of V (III) and V (II) solutions in sulfuric acid solution for vanadium battery applications, Ph.D. Thesis, UNSW, 2003.
[17] http://www.engineeringtoolbox.com/thermal-conductivity-d_429.html. (last accessed: Mar. 2012).
[18] M. Kazacos, M. Cheng, M. Skyllas-Kazacos, J. Appl. Electrochem. 20 (1990) 463–467.
[19] J. Xi, Z. Wu, X. Qiu, L. Chen, J. Power Sources 166 (2007) 531–536.
[20] Q. Luo, H. Zhang, J. Chen, P. Qian, Y. Zhai, J. Memb. Sci. 311 (2008) 98–103.
[21] G. Hu, Y. Wang, J. Ma, J. Qiu, J. Peng, J. Li, M. Zhai, J. Memb. Sci. 407–408 (2012) 184–192.
[22] W. Wei, H. Zhang, X. Li, Z. Mai, H. Zhang, J. Power Sources 208 (2012) 421–425.